Novel cystine transporter in renal proximal tubule identified as a missing partner of cystinuria-related plasma membrane protein rBAT/SLC3A1

Shushi Nagamori[a], Pattama Wiriyasermkul[a,1], Meritxell Espino Guarch[b,c,d,1], Hirohisa Okuyama[a], Saya Nakagomi[a], Kenjiro Tadagaki[a], Yumiko Nishinaka[a], Susanna Bodoy[b,d], Kazuaki Takafuji[a], Suguru Okuda[a], Junko Kurokawa[e], Ryuichi Ohgaki[a], Virginia Nunes[c,d,f], Manuel Palacín[b,d,g], and Yoshikatsu Kanai[a,2]

[a]Department of Bio-System Pharmacology, Graduate School of Medicine, Osaka University, Suita, Osaka 565-0871, Japan; [b]Institute for Research in Biomedicine Barcelona, The Barcelona Institute of Science and Technology, 08028 Barcelona, Spain; [c]Molecular Genetics Laboratory, Institut d'Investigació Biomèdica de Bellvitge, L'Hospitalet de Llobregat, 08908 Barcelona, Spain; [d]Spanish Biomedical Research Center in Rare Diseases (CIBERER), 08028 Barcelona, Spain; [e]Department of Bio-Informational Pharmacology, Medical Research Institute, Tokyo Medical and Dental University, Tokyo 113-8510, Japan; [f]Genetic Unit, Department of Physiological Sciences II, Universitat de Barcelona, 08908 Barcelona, Spain; and [g]Department of Biochemistry and Molecular Biology, Facultat de Biologia, University of Barcelona, 08028 Barcelona, Spain

Edited by David W. Russell, University of Texas Southwestern Medical Center, Dallas, TX, and approved December 11, 2015 (received for review October 8, 2015)

Heterodimeric amino acid transporters play crucial roles in epithelial transport, as well as in cellular nutrition. Among them, the heterodimer of a membrane protein $b^{0,+}$AT/SLC7A9 and its auxiliary subunit rBAT/SLC3A1 is responsible for cystine reabsorption in renal proximal tubules. The mutations in either subunit cause cystinuria, an inherited amino aciduria with impaired renal reabsorption of cystine and dibasic amino acids. However, an unsolved paradox is that rBAT is highly expressed in the S3 segment, the late proximal tubules, whereas $b^{0,+}$AT expression is highest in the S1 segment, the early proximal tubules, so that the presence of an unknown partner of rBAT in the S3 segment has been proposed. In this study, by means of coimmunoprecipitation followed by mass spectrometry, we have found that a membrane protein AGT1/SLC7A13 is the second partner of rBAT. AGT1 is localized in the apical membrane of the S3 segment, where it forms a heterodimer with rBAT. Depletion of rBAT in mice eliminates the expression of AGT1 in the renal apical membrane. We have reconstituted the purified AGT1-rBAT heterodimer into proteoliposomes and showed that AGT1 transports cystine, aspartate, and glutamate. In the apical membrane of the S3 segment, AGT1 is suggested to locate itself in close proximity to sodium-dependent acidic amino acid transporter EAAC1 for efficient functional coupling. EAAC1 is proposed to take up aspartate and glutamate released into luminal fluid by AGT1 due to its countertransport so that preventing the urinary loss of aspartate and glutamate. Taken all together, AGT1 is the long-postulated second cystine transporter in the S3 segment of proximal tubules and a possible candidate to be involved in isolated cystinuria.

amino acid transporter | cystine reabsorption | cystinuria | kidney

The heteromeric amino acid transporter (HAT) family is one of the major amino acid transporter families responsible for cellular uptake and epithelial transport (1–3). HATs form heterodimers composed of a 12 membrane spanning light chain (SLC7) that catalyzes transport functions and a single membrane spanning heavy chain (SLC3) essential for plasma membrane localization and stabilization of the light chains. Two heavy chains, SLC3A1/rBAT and SLC3A2/4F2hc/CD98hc, covalently bound to light chains via a disulfide bridge have been identified so far (4–6). 4F2hc interacts with most of the light chains in HATs whereas rBAT has been known to form a heterodimer only with $b^{0,+}$AT/SLC7A9. Because the rBAT-$b^{0,+}$AT complex is presented on the apical membrane of proximal tubules in the kidney and involved in the reabsorption of cystine and dibasic amino acids, the mutations of either rBAT or $b^{0,+}$AT cause cystinuria, a disorder of renal reabsorption of cystine and dibasic amino acids leading to serious renal lithiasis due to low solubility of cystine (7).

An unsolved paradox on rBAT and $b^{0,+}$AT has been the discrepancy between the distribution of rBAT and that of $b^{0,+}$AT (5, 8–10). rBAT is the most abundant in the S3 segment of proximal tubules, and its expression declines toward the S1 segment (11, 12). In contrast, the expression of $b^{0,+}$AT is highest in the S1 segment and decreases toward the S3 segment (5, 8). Furthermore, even in $b^{0,+}$AT-deficient mice, heterodimers containing rBAT still have been observed (13). Therefore, it has been proposed that unknown partners of rBAT exist in the S3 segment (5, 9, 14, 15).

The HAT family includes two members, AGT1/SLC7A13 and Asc2, whose heavy chains have not been identified (16, 17). Among them, aspartate/glutamate transporter 1 (AGT1) has been identified as an Na^+-independent acidic amino acid transporter expressed specifically in the kidney (17). In this study, we have generated new anti-AGT1 antibodies to search for the unknown heavy chain(s), by means of coimmunoprecipitation followed by mass spectrometry, and have revealed that rBAT is a heavy chain of AGT1. AGT1 was detected at the apical membrane of the S3 segment in renal proximal tubules. A transport assay of the AGT1-rBAT heterodimer reconstituted into proteoliposomes revealed that it transports cystine as well as aspartate and glutamate. We

Significance

Although molecular identification of transporters in mammals seems almost settled, some long-proposed transporters still remain to be revealed. The second cystine transporter in renal cystine reabsorption is one of such transporters. Its genetic defect has been proposed to be responsible for a type of cystinuria distinct from that caused by the mutations of the already known cystine transporter. In this study, we have found a membrane protein SLC7A13 as the second cystine transporter with proposed characteristics, and provided a possible clue to the genetics of previously unidentified cystinuria. Intricate functional coupling of SLC7A13 with the nearby glutamate transporter is also proposed. We have solved long-lasting problems in renal cystine transport physiology and paradoxes regarding the unmatched distribution of cystine transporter components.

Author contributions: S. Nagamori, V.N., M.P., and Y.K. designed research; S. Nagamori, P.W., M.E.G., H.O., S. Nakagomi, K. Tadagaki, Y.N., S.B., K. Takafuji, S.O., J.K., and R.O. performed research; S. Nagamori, P.W., M.E.G., V.N., M.P., and Y.K. analyzed data; and S. Nagamori and Y.K. wrote the paper.

The authors declare no conflict of interest.

This article is a PNAS Direct Submission.

Freely available online through the PNAS open access option.

[1]P.W. and M.E.G. contributed equally to this work.

[2]To whom correspondence should be addressed. Email: ykanai@pharma1.med.osaka-u.ac.jp.

This article contains supporting information online at www.pnas.org/lookup/suppl/doi:10.1073/pnas.1519959113/-/DCSupplemental.

PHYSIOLOGY

conclude that AGT1 is a strong candidate for the "missing partner" of rBAT and a second cystine transporter in the kidney.

Results

Identification of a Heavy Chain for AGT1. Anti-AGT1 antibodies were newly generated against C-terminal 24 amino acid peptides. The specificities of the antibodies, anti-AGT1(M) and anti-AGT1(G) (*SI Materials and Methods*), were confirmed using 3xFLAG-tagged AGT1 as shown in Fig. S1. In Western blot, the antibodies specifically recognized a band for AGT1 in the male kidney but not in the female (Fig. 1*A*). mRNA for AGT1 was also detected only in the male kidney by semiquantitative RT-PCR (Fig. S2*A*). There are no perfect palindrome estrogen (ERE) and androgen (ARE) response elements in the 10 kbp upstream of the *AGT1* gene, as well as in the *AGT1* gene on mouse chromosome 4. Instead, three imperfect palindrome AREs and a lot of half sites of ARE and ERE were found in the regions (Fig. S2*B*).

AGT1 migrated at ~40 kDa in the reducing condition whereas the bands around 140 kDa and over 240 kDa were detected in the nonreducing condition (Fig. 1*A*). The band shift from 140 kDa to 40 kDa was presumably due to the breakage of a disulfide bridge between AGT1 and its heavy chain in the reducing condition. The band over 240 kDa seems to be oligomers of heteromeric complexes similar to those observed for HATs (5, 18–20).

To identify the unknown partner of AGT1, AGT1 was immunoprecipitated using anti-AGT1 antibodies (Fig. S3*A*). The elution fraction containing AGT1 in the immunoprecipitation was subjected to shotgun mass spectrometry. In all of the independent experiments [three times with anti-AGT1(M) and once with anti-AGT1(G)], rBAT was detected with high protein scores (21) (Fig. S3*B*). At the best, 19 peptides were identified on the rBAT amino acid sequence, which covered 31.7% of the protein. Peptides corresponding to AGT1 were also detected by mass spectrometry. None of the peptides corresponding to 4F2hc or $b^{0,+}$AT were detected. In addition, none of the rBAT peptides were identified from samples precipitated with normal rabbit IgG.

To confirm rBAT as a partner of AGT1, immunoprecipitated samples were analyzed by Western blot. As shown in Fig. 1*B*, rBAT was detected after immunoprecipitation using anti-AGT1 antibody, but not with normal IgG. Moreover, AGT1 was detected by immunoprecipitation with anti-rBAT antibody (Fig. 1*B*). After overnight incubation for immunoprecipitation in the presence of detergent, AGT1 appeared more abundantly as homodimers (around 70 kDa in Fig. 1*B*, *Right* and Fig. S3*A*) than monomers (35–40 kDa in Fig. 1*B*, *Right* and Fig. S3*A*) whereas monomeric AGT1 was mainly detected in freshly prepared proteins (Fig. 1*A* and Fig. S3*A*).

To further confirm rBAT as an AGT1 partner, the expression of AGT1 was examined in mice carrying a missense mutation in rBAT causing the loss of rBAT protein in brush-border membrane vesicles (BBMVs) (Fig. 1*C*, *Right*) (10, 22). In the mutant mice, the band corresponding to the complex of AGT1 and its heavy chain detected by anti-AGT1 antibody was diminished in BBMVs, supporting the idea that rBAT is the heavy chain of AGT1 (Fig. 1*C*, *Left*). The Western blots of BBMVs (Fig. 1*C*) and crude membrane fractions from WT mouse kidney (Fig. 1 and Fig. S3*C*) indicate that rBAT protein, as well as AGT1, is more abundant in male than female whereas the amount of $b^{0,+}$AT has no biological sex difference (Fig. S3*C*). The AGT1-rBAT heterodimer and $b^{0,+}$AT-rBAT heterodimer were distinguishable by Western blot using anti-rBAT antibody because the AGT1-rBAT heterodimer did not exist in the female kidney (Fig. S3*C*).

One of the known functions of heavy chains of HATs is to localize the light chains to the plasma membrane (19, 23–26). To examine the role of rBAT in the localization of AGT1, AGT1 was expressed with rBAT in HEK293 cells. As shown in Fig. S4 *A–C*, expression of 3xFLAG-AGT1, rBAT, or 4F2hc alone resulted in the intracellular localization. In contrast, when 3xFLAG-AGT1 and rBAT were coexpressed, they both were localized on the plasma membrane (Fig. S4 *D–F*). 4F2hc, the other heavy chain of HATs, did not support membrane localization of 3xFLAG-AGT1 (Fig. S4 *G–I*).

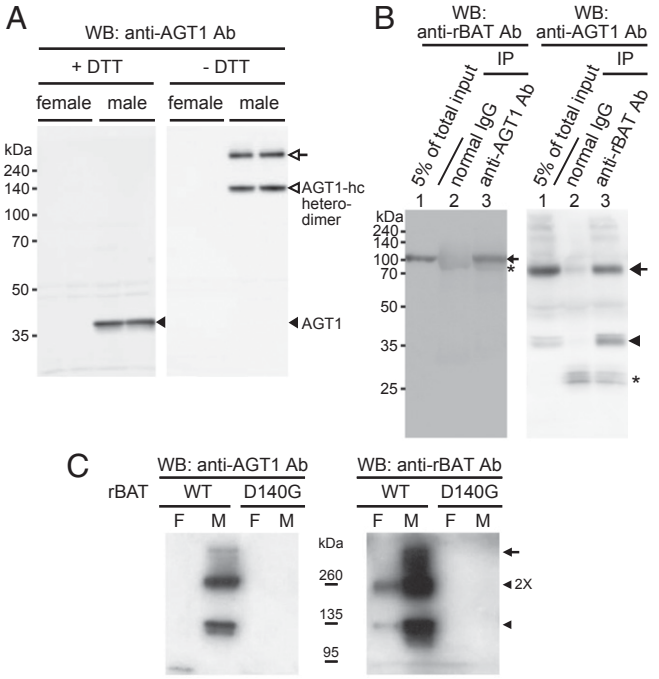

Fig. 1. AGT1-heavy chain heterodimer in mouse kidney. (*A*) Expression of AGT1 in kidney. Western blot was performed on crude membrane fractions from two female and two male mice using the anti-AGT1(M) antibody. Western blots (*Left* and *Right*) were performed in the presence (+DTT) or absence (– DTT) of 100 mM DTT, respectively. Filled arrowheads indicate AGT1. Open arrowhead points to heterodimers of AGT1 and its heavy chain (AGT1-hc heterodimer) whereas the open arrow indicates the oligomeric complex. (*B*) Immunoprecipitation on renal brush-border membrane vesicles (BBMVs) with the anti-AGT1(M) antibody or anti-rBAT antibody. Western blot was performed with the anti-rBAT antibody or anti-AGT1(M) antibody in the presence of 100 mM DTT. The small arrow (*Left*) and the arrowhead (*Right*) indicate the bands for rBAT and AGT1, respectively. The large arrow (*Right*) indicates the AGT1 homodimer. Normal rabbit IgG was used as a control for immunoprecipitation. Asterisks are the bands derived from IgG. (*C*) Expression of AGT1 and rBAT in the mutant mouse kidney Western blot was performed on renal BBMVs from different genotypes [WT (*Slc7a9*$^{+/+}$ and *Slc3a1*$^{+/+}$) and D140G (*Slc3a1* missense mutation)] of male (M) and female (F) mice in the nonreducing condition. The anti-AGT1(G) and anti-rBAT antibodies detected AGT1-rBAT heterodimer (arrowhead) and its oligomers, including dimers of heterodimeric complexes (arrowhead 2×) and higher oligomeric complexes (arrow).

Localization of Expression of AGT1 in Mouse Kidney. Immunohistochemical analysis of the male mouse kidney using an anti-AGT1(G) antibody revealed strong AGT1 immunoreactivity on the renal tubules in the outer stripe of the outer medulla and medullary ray (Fig. 2 *A* and *B*). The AGT1 protein was mainly localized on the apical membrane of the tubules (Fig. 2 *B* and *C*). No staining was detected in the female mouse kidney by the anti-AGT1(G) antibody (Fig. S5 *A–C*). The localization of AGT1 in the male mouse kidney was confirmed by the anti-AGT1(M) antibody (Fig. S5 *D–F*). The localization of AGT1 was further confirmed by in situ hybridization showing a similar pattern of positive signals in the male mouse kidney and no signal in the female kidney (Fig. S6). Structured illumination microscopy (SIM) revealed AGT1 immunoreactivity at the surface of apical membranes, which is evident compared with the fluorescence from apical membrane staining marker lectin phytohemagglutinin-L (PHA-L) (Fig. 2 *D–F*).

Colocalization of AGT1 and rBAT in the mouse kidney was demonstrated by immunofluorescence double staining (Fig. 2 *G–L*). Consistent with the results from immunohistochemistry in Fig. 2*A*, AGT1 immunofluorescence signals dominantly appeared on the

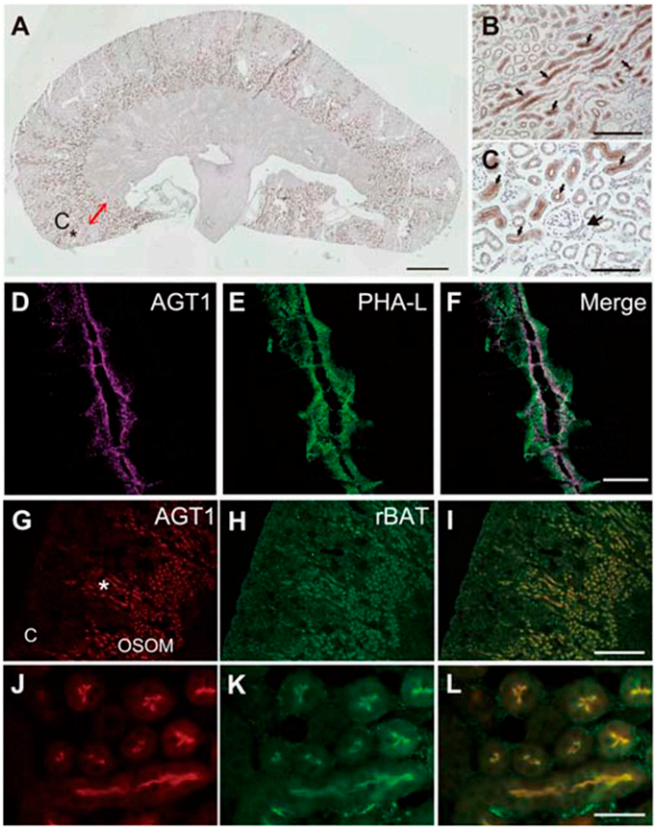

Fig. 2. Localization of AGT1 and rBAT in the male mouse kidney. (*A–C*) Localization of AGT1 in immunohistochemistry. AGT1 immunoreactivity was detected on the renal tubules located in the outer stripe of the outer medulla (red two-way arrow in *A*) and medullary ray (asterisk in *A* and arrows in *B*) in low and middle magnification views (*A* and *B*). The "C" in *A* indicates the renal cortex. AGT1 immunoreactivity was localized on the apical membrane of the tubules (small arrows in *C*). AGT1 immunoreactivity was less detected in distal convoluted tubules characterized by macula densa (large arrow in *C*). (Scale bars: *A*, 1 mm; *B*, 200 μm; *C*, 100 μm.) (*D–F*) Structured illumination microscopy (SIM) analysis of AGT1. The AGT1 signal is shown in cyan (*D*) whereas the signal for lectin PHA-L used as an apical membrane marker is shown in green. Their merged image is shown in *F*. (Scale bar: 10 μm.) (*G–L*) Coimmunofluorescence staining of AGT1 and rBAT on the apical membrane of renal tubules. Low magnification views indicate the colocalization of AGT1 and rBAT on the tubules in the outer stripe of the outer medulla ("OSOM" in *G*) and medullary ray (asterisk in *G*). (*G–I*) The "C" in *G* indicates the renal cortex. AGT1 and rBAT are colocalized on the apical membrane of the tubules in high magnification views (*J–L*). Signals for AGT1 and rBAT are shown in red (*G* and *J*) and green (*H* and *K*), respectively. Merged images are shown in *I* and *L*. (Scale bars: *I*, 500 μm; *L*, 25 μm.) The anti-AGT1(G) antibody was used for immunohistochemistry and immunofluorescence experiments.

renal tubule in the outer stripe of the outer medulla and medullary ray (Fig. 2*G*). In contrast, rBAT immunoreactivity was extended to the superficial cortex although that in the outer stripe of the outer medulla and medullary ray was the strongest (Fig. 2*H*), as reported previously (11, 12). The immunoreactivity of AGT1 was completely merged with that of rBAT at the apical membrane of the proximal tubules (Fig. 2 *J–L*).

Functional Characterization of AGT1 in Proteoliposome. Functional properties of the AGT1-rBAT heterodimer were examined by reconstitution into proteoliposomes. AGT1 and rBAT were stably coexpressed in HEK293 cells and purified as a complex (Fig. S7). Most of the purified AGT1 formed heterodimers with rBAT. $b^{0,+}$AT was not detected in any fractions, including the elution fraction (Fig. S7). The AGT1-rBAT proteoliposomes preloaded with or without aspartate were incubated with [^{14}C]cystine (Fig. 3*A*). Although the control liposomes did not accumulate radioactivity, time-dependent increase of [^{14}C]cystine uptake was observed in AGT1-rBAT proteoliposomes without aspartate inside (Fig. 3*A*), indicating that the AGT1-rBAT heterodimer mediated downhill cystine influx. Such a facilitative transport of cystine displayed a hyperbolic dependence on cystine concentration, fitted to the Michaelis–Menten equation with a K_m value of 67.6 μM. In contrast, the proteoliposomes preloaded with aspartate exhibited a higher initial rate of [^{14}C]cystine influx. The accelerated influx was transient, and the uptake peaked at around 10 min, after which the accumulated radioactivity declined gradually (Fig. 3*A*). This overshoot is typical of active transport driven by cotransport or countertransport in proteoliposome (27). It suggests that AGT1-rBAT heterodimer mediates countertransport when counter substrates exist. The countertransport mediated by AGT1-rBAT was confirmed by efflux experiments in which [^{14}C]cystine was preloaded into proteoliposomes. The efflux of [^{14}C]cystine was estimated in the presence or absence of external aspartate by measuring the radioactivity remaining in the proteoliposomes. As shown in Fig. 3*B*, the efflux of preloaded cystine was accelerated by external aspartate in a concentration-dependent manner.

The ion dependence of the transport was examined for the countertransport mode in the condition that aspartate and K^+ (150 mM) were loaded into the AGT1-rBAT proteoliposomes. The proteoliposomes were incubated with Na^+ (150 mM) or K^+ (150 mM). As shown in Fig. 3*C*, the influx of both cystine and aspartate was not significantly dependent on Na^+.

The substrate selectivity of the AGT1-rBAT heterodimer was examined for the countertransport mode on the proteoliposomes preloaded with aspartate. As shown in Fig. 3*D*, a high level of influx was observed for aspartate, glutamate, and cystine whereas a lower level of influx was detected for glutamine, leucine, methionine, phenylalanine, valine, tyrosine, and tryptophan. Serine, cysteine, and basic amino acids, such as lysine and arginine, were not transported. To differentiate its substrate recognition from that of other acidic amino acid transporters, the effects of acidic amino acid analogs (see structures in Fig. S8) were investigated on [^{14}C]aspartate influx. As shown in Fig. 3*E*, *threo*-β-hydroxyaspartate and cysteine sulfinate inhibited [^{14}C]aspartate uptake as well as aspartate and glutamate did whereas the inhibition by serine-*O*-sulfate, cysteate, cysteine, and homocysteine was less than that by aspartate and glutamate. In contrast, α-aminoadipate, homocysteate, *trans*-pyrrolidine-2,4-dicarboxylate, and dihydrokainate did not inhibit the uptake. Cystine exhibited a similar level of inhibition compared with aspartate and glutamate.

Colocalization of AGT1 with Acidic Amino Acid Transporter EAAC1 (SLC1A1). In the mouse kidney, EAAC1 was detected by immunofluorescence microscopy in the cortex and outer stripe of the outer medulla, where the outer stripe of the outer medulla and medullary ray exhibited stronger fluorescence than the superficial cortex (Fig. 4*A*). EAAC1 immunoreactivity was detected at the apical membranes of tubules by SIM (Fig. 4*B*), similar to AGT1 (Fig. 4*C*). AGT1 immunoreactivity was colocalized with the staining of EAAC1 (Fig. 4 *D* and *E*) whereas the tubules expressing EAAC1 but not AGT1 also exist due to the wider distribution of EAAC1 in proximal tubules (Fig. 4*E*). To further investigate the spatial relation of AGT1 and EAAC1, the distance between the two molecules was estimated with an in situ proximity ligation assay. In this assay, the fluorescence signal is detected only when two target proteins are in close proximity to each other: The theoretical maximum distance between two target proteins is 30–40 nm (28). Kidney sections reacted with both the anti-AGT1 antibody and anti-EAAC1 antibody showed positive red fluorescent signals, suggesting that AGT1 and EAAC1 are closely placed with each other (Fig. 5*A*) whereas no signal was detected in the kidney sections treated with only either the anti-AGT1 antibody or anti-EAAC1 antibody (Fig. 5 *B* and *C*). The treatment with the anti-AGT1 antibody and anti-rBAT antibody produced positive signals as well as the combination of the anti-$b^{0,+}$AT antibody and anti-rBAT antibody whereas positive signals were not detected

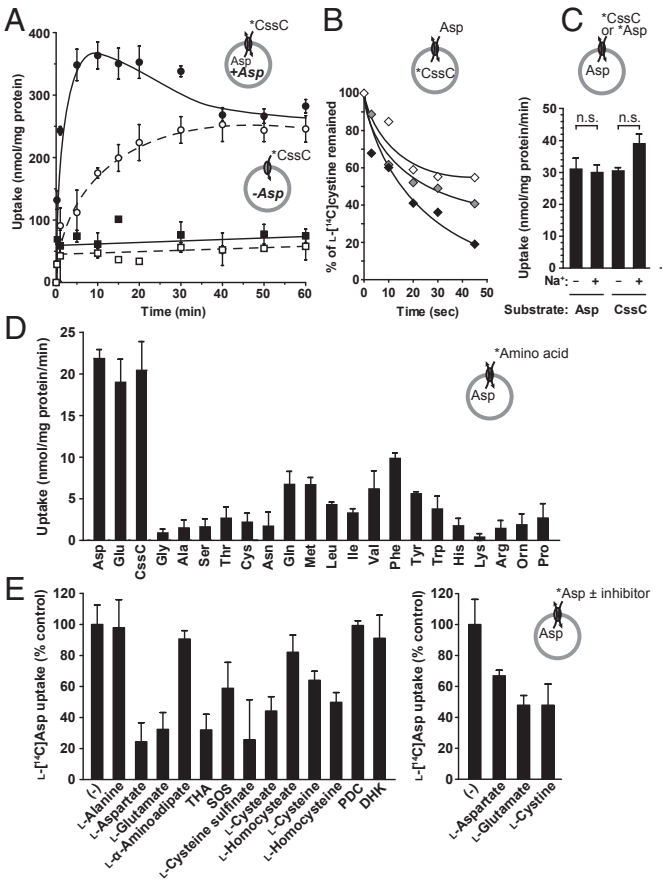

Fig. 3. Functional analysis of the AGT1-rBAT heterodimer in proteoliposomes. (*A*) Time course of downhill cystine influx and cystine countertransport. The proteoliposomes reconstituted with the AGT1-rBAT heterodimer and preloaded with (filled circle) or without (open circle) 4 mM aspartate, as well as control liposomes preloaded with (filled square) or without (open square) 4 mM aspartate, were incubated in 100 μM [^{14}C]cystine. CssC, cystine; *CssC, [^{14}C]cystine. (*B*) The effect of external aspartate on cystine efflux. The efflux of [^{14}C]cystine (100 μM) was evaluated in the absence (open diamond) or presence of external nonradioactive aspartate (gray diamond, 100 μM; filled diamond, 500 μM). The radioactivity remaining in the proteoliposomes was shown as percent of loaded radioactivity. (*C*) Ion dependence of the transport. The uptake of [^{14}C]cystine and [^{14}C]aspartate (100 μM) was measured for 10 min in sodium uptake buffer (+) or potassium uptake buffer (–). The proteoliposomes were preloaded with 4 mM aspartate. *Asp, [^{14}C]aspartate. Statistical difference was determined using the Student's unpaired *t* test. Differences were considered significant at $P < 0.05$. (*D*) Substrate selectivity of AGT1. Proteoliposomes loaded with 4 mM aspartate were incubated in sodium uptake buffer containing ^{14}C-labeled amino acids (100 μM) for 10 min. *Amino acid, radiolabeled L-amino acid. (*E*) The effects of acidic amino acid analogs on the transport. The uptake of 20 μM [^{14}C]aspartate into the proteoliposome loaded with 4 mM aspartate was measured for 5 min in the presence or absence (–) of indicated compounds. The test compounds (*Left*) were at 5 mM except *threo*-β-hydroxyaspartate (THA) (2 mM). The compounds in the *Right* were at 0.5 mM. DHK, dihydrokainate; PDC, L-*trans*-pyrrolidine-2,4-dicarboxylate; SOS, L-serine-*O*-sulfate. The uptake values shown in *C*–*E* are the influx into proteoliposomes minus the influx into control liposomes. The potassium uptake buffer was used for *A*, *B*, and *E*. All data in Fig. 3, except *B*, represent mean ± SE; $n = 3$–4.

when the anti-AGT1 antibody was combined with an antibody for CD13/aminopeptidase N, localized at the apical membrane of the proximal tubules (Fig. 5 *D*–*F*).

Discussion

On the cystine reabsorption in the renal proximal tubule, a long-standing issue that has not been solved since the discovery of rBAT and $b^{0,+}$AT is the discrepancy regarding the distribution of rBAT and $b^{0,+}$AT along the renal proximal tubules. Based on this discrepancy, it has been postulated that rBAT has an unknown partner other than $b^{0,+}$AT. It should be the main rBAT-partner in the S3 segment of the proximal tubules where the expression of $b^{0,+}$AT is substantially low whereas that of rBAT is the highest. In an attempt to reveal an unidentified heavy chain of AGT1 in the present study, we have found that AGT1 is the long-awaited rBAT-partner in the S3 segment.

By means of immunoprecipitation using anti-AGT1 antibodies followed by mass spectrometry, rBAT was identified as a binding partner of AGT1. rBAT associates with AGT1 via a disulfide bond (Fig. 1) and translocates AGT1 to the plasma membrane, consistent with the proposed role of heavy chains of HATs. In the kidney, AGT1 expression is largely restricted to the outer stripe of the outer medulla and medullary ray where it is colocalized with the strongest staining of rBAT. It indicates that AGT1 is present in the S3 segment of the proximal tubules because the strong rBAT staining is a marker for the S3 segment (11). The presence of the AGT1-rBAT heterodimer in the proximal tubules was supported by an in situ proximity ligation assay (Fig. 5*D*) and further was confirmed by the observation that AGT1 disappeared from the BBMV in mutant mice lacking rBAT expression (Fig. 1*C*). Therefore, we concluded that AGT1 is the transporter corresponding to the missing partner of rBAT in the S3 segment of the proximal tubules. Additionally, we found a remarkable biological-sex difference in the expression of AGT1 in the kidney. Although we could not find perfect palindrome estrogen (ERE) and androgen (ARE) response elements associated with the *AGT1* gene (Fig. S2*B*), some of the imperfect palindrome AREs and/or half-sites of ARE and ERE could be involved in male-specific AGT1 expression. The functional significance of imperfect AREs and half-sites of ARE or ERE is, however, still not established (29).

In this study, the localization of AGT1 was examined by two newly generated antibodies raised against the C-terminal intracellular domain of AGT1 produced by expressing it in *Escherichia coli*. In the immunohistochemistry of mouse kidney cryosections, basically identical results were obtained by using these two antibodies on the localization of AGT1 (Fig. 2 and Fig. S5), which was further confirmed by in situ hybridization (Fig. S6). Using these antibodies, AGT1 was localized to the apical membrane of the S3 segment (Fig. 2). In a previous study, an antiserum raised against a synthetic oligo peptide corresponding to the predicted amino acid sequence of AGT1 stained the basolateral membrane of proximal straight tubules and distal convoluted tubules in mouse kidney paraffin sections (17). Although the staining was eliminated in the absorption experiments using the antigen peptide, it is possible that the antibody recognized epitopes in tissue sections other than AGT1.

For functional analyses using *Xenopus* oocytes in the previous study, we generated fusion proteins in which AGT1 was connected with 4F2hc or rBAT to ensure plasma membrane sorting (17). Both fusion proteins expressed Na^+-independent transport for aspartate and glutamate although their uptake levels were low. Because such fusion of proteins may affect the function, we purified an AGT1-rBAT heterodimer (Fig. S7) and reconstituted it into proteoliposomes. This proteoliposome reconstitution allowed us to examine the function of the heterodimer, avoiding distortion by protein fusions and excluding possible effects from other proteins, amino acids, and inorganic ions in the cells.

By proteoliposome reconstitution, we have revealed that the AGT1-rBAT heterodimer transports cystine as well as aspartate and glutamate. In the previous study, cystine transport activity was not detected for the fusion proteins in *Xenopus* oocytes although cystine weakly inhibited aspartate uptake (17). In addition, the AGT1-rBAT heterodimer also mediated a lower level of transport of some neutral amino acids, which was not detected in the fusion proteins. The profile of inhibition of [^{14}C]aspartate uptake by acidic amino acid analogs for the AGT1-rBAT heterodimer in proteoliposome shown in Fig. 3*E* was similar to that for the AGT1-4F2hc fusion protein (17). AGT1 would recognize cystine as an anionic amino acid similar to other HAT member

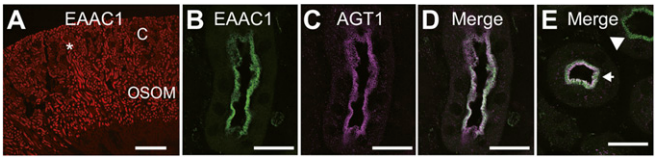

Fig. 4. Localization of AGT1 with acidic amino acid transporter EAAC1 in the male mouse kidney. (*A*) Localization of EAAC1 in immunofluorescence microscopy. EAAC1 immunoreactivity was detected strongly in the outer stripe of the outer medulla ("OSOM") with the medullary ray (asterisk). Weaker staining was also detected in the cortex ("C"). (Scale bar: 500 μm.) (*B–E*) Coimmunofluorescence staining of EAAC1 and AGT1 on the apical membrane of renal tubules in SIM analysis. EAAC1 and AGT1 signals are shown in green and cyan, respectively. A merged image of *B* and *C* is shown in *D*. *E* was merged from other independent pictures. AGT1 was colocalized with EAAC1 (arrow) whereas tubules expressing EAAC1 but not AGT1 (arrow head) also exist (*E*). (Scale bars: *D* and *E*, 20 μm.) The anti-AGT1(G) antibody was used for immunofluorescence experiments.

xCT/SLC7A11 that transports glutamate and cystine by recognizing cystine as an anionic amino acid. AGT1 is, however, still distinct from xCT in that AGT1 transports aspartate with a short side chain and escapes α-aminoadipate with a longer side chain (Fig. 3*E*), suggesting that AGT1 prefers anionic amino acids with shorter side chains.

In the apical membrane of the proximal tubule S3 segment, we have found that AGT1 is colocalized with Na^+-dependent acidic amino acid transporter EAAC1 (30, 31) (Fig. 4). An in situ proximity ligation assay strongly suggests that they are present in the immediate vicinity of each other (Fig. 5). Such a colocalization in close proximity would enable efficient functional coupling between two transporters with overlapping substrates. As depicted in Fig. S9, aspartate and glutamate would be released into the luminal fluid via AGT1 when AGT1 reabsorbs substrates, including cystine, from the luminal fluid. The released aspartate and glutamate could be taken up and salvaged by closely located EAAC1 to prevent their urinary loss. The cystine taken up by AGT1 is converted to cysteine in the cytoplasm of epithelial cells, which ensures directional flow of cystine from tubular fluid to the cytoplasm of tubular epithelial cells. Therefore, it is proposed that AGT1 and EAAC1 in concert function as a cystine reabsorption system as a whole using aspartate and glutamate as internal-coupling substrates (Fig. S9). Through such cooperation, EAAC1 may furthermore drive and boost AGT1 by providing aspartate and glutamate to the intracellular substrate-binding site of AGT1, particularly when enough concentration of counter substrates is not available at the intracellular surface of the plasma membrane.

Two distinct cystine transport systems were once reported in the rodent kidney (32). One of them had no interaction with dibasic amino acids, which corresponds well with the AGT1-rBAT heterodimer characterized in the present study. An additional feature of such a cystine transport system described in BBMV was that its transport activity is increased in the presence of Na^+. In our present study, Na^+ dependence was not significant in the proteoliposome (Fig. 3*C*). It might be possible that some Na^+-dependent transporters such as Na^+-dependent acidic amino transporter EAAC1 as described above could cooperate and provide AGT1 with counter substrates to drive it, which makes the cystine transport somewhat Na^+-dependent. It is reminiscent of the renal urate reabsorption system in which Na^+-dependent monocarboxylate transporters provide counter substrates and drive Na^+-independent urate transporter URAT1 to confer Na^+ dependence on the urate reabsorption system (33).

In the physiological condition, more than 90% of cystine is reabsorbed in early proximal tubules, where $b^{0,+}$AT is the partner of rBAT, leaving a small portion of cystine to be reabsorbed by AGT1-rBAT. The small contribution to cystine reabsorption proposed for AGT1-rBAT may explain why cystine is not increased in the urine in dicarboxylic amino aciduria that is caused by the dysfunction of EAAC1 (34) although EAAC1 is supposed to drive AGT1 in some conditions as discussed above. However, when $b^{0,+}$AT is defective in mice, the fractional excretion of cystine is only 11%, and the remaining cystine reabsorption has been attributed to uncharacterized cystine transport (35). The small fractional excretion of cystine in $b^{0,+}$AT-defective mice suggests that cystine transporters other than $b^{0,+}$AT possess high reserve capacity to compensate largely the loss of $b^{0,+}$AT function, similar to the renal glucose reabsorption system in which SGLT1 in late proximal tubules makes up the glucose reabsorption by means of its high reserve capacity when SGLT2 in early proximal tubules is inhibited (36, 37). In fact, in the digenic inheritance of cystinuria mice, it was reported that the prevalence and severity of lithiasis are increased in the double homozygote ($Slc7a9^{-/-}Slc3a1^{-/-}$) compared with the single one ($Slc7a9^{-/-}Slc3a1^{+/+}$) (10), which supports the significant contribution of the heterodimer of rBAT and a light chain other than $b^{0,+}$AT to tubular cystine reabsorption. Notably, cystinuria patients who have no urinary hyperexcretion of dibasic amino acids were found in a German family and a British family (38, 39), as well as in dogs (40). Although the mutation T123M in $b^{0,+}$AT was reported for patients from the German family with such isolated cystinuria (38), AGT1 mutations might also explain additional cases of this type of cystinuria.

Taken all together, the evidence strongly suggests that the AGT1-rBAT heterodimer corresponds to a transport system involved in cystine reabsorption in renal proximal tubules. The identification of this second cystine transporter in proximal tubules has answered long-lived questions regarding cystine reabsorption. Simultaneously, it raises a series of new questions, such as the actual physiological contribution of AGT1 in renal cystine reabsorption, the biological sex difference in AGT1 expression, and the relevance of AGT1 to cystinuria, that require further studies to address these subjects.

Materials and Methods

SI Materials and Methods includes additional information on experimental methods.

Animal Studies. All studies were approved by the Osaka University Animal Care and Use Committee and the Committee for the Use and Care of Animals in Institut d'Investigació Biomèdica de Bellvitge.

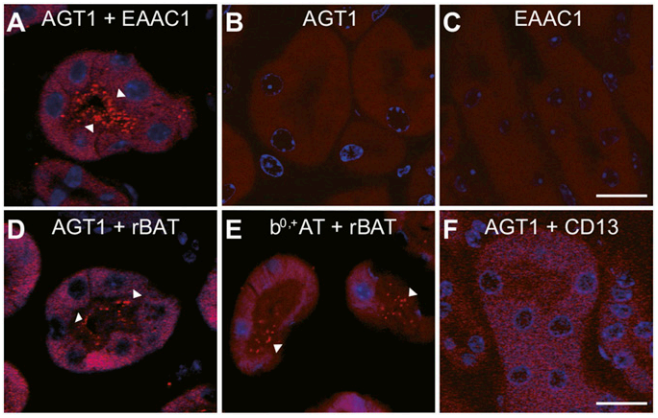

Fig. 5. Colocalization of AGT1 and EAAC1 determined by proximity ligation assay. An in situ proximity ligation assay (PLA) was performed on male mouse kidney sections. In the confocal images of the mouse kidney sections, positive PLA fluorescence signals are shown in red (arrowheads). Nuclei were stained with DAPI (blue). The positive signals were detected on the brush border region of proximal tubules treated with both anti-AGT1(G) and anti-EAAC1 antibodies (*A*). No signals were seen in the sections treated with anti-AGT1 antibody alone or anti-EAAC1 antibody alone (*B* and *C*). Positive PLA fluorescence signals were also obtained between $b^{0,+}$AT and rBAT (*D*) and between AGT1 and rBAT (*E*). No positive signal was seen in the sections treated with anti-AGT1 and anti-CD13 antibodies (*F*). (Scale bars: 10 μm.)

Antibodies, Immunoprecipitation, and Mass Spectrometry. Anti-AGT1 antibodies were newly generated in this study as described in *SI Materials and Methods*. Immunoprecipitation of AGT1 or rBAT was performed, and the immunoprecipitated proteins were subjected to mass spectrometry to identify a heavy chain for AGT1 (*SI Materials and Methods*).

Immunohistochemistry and Immunofluorescence Microscopy. Immunohistochemistry and immunofluorescence microscopy were performed as described in *SI Materials and Methods*. Superresolution SIM images were obtained by using an Elyra S1 microscope (Carl Zeiss). A duolink in situ proximity ligation assay (PLA) (Sigma-Aldrich) was used according to the manufacturer's protocol.

Transport Assays on Proteoliposomes. rBAT and 3xFLAG-AGT1 were purified as a heterodimeric complex and reconstituted into proteoliposomes by the dilution-freeze/thaw method (41). The proteoliposomes were subjected to transport assays as described in *SI Materials and Methods*.

ACKNOWLEDGMENTS. We thank Michiko Minobe, Maya Hakozaki, Fu Okajima, Takanori Kobayashi, and Yoko Tanaka for technical assistance and Ryo Hatano, Atsushi Sato, and Kenichiro Iio for help with research. This work was supported in part by Grants-in-Aid for Scientific Research on Priority Areas of "Transportsome" (to Y.K.) and Innovative Areas "HD Physiology" (to S. Nagamori) from the Ministry of Education, Culture, Sports, Science and Technology of Japan; Grants-in-Aid for Scientific Research (to Y.K. and S. Nagamori) from the Japan Society for the Promotion of Science; a research grant from the Japanese Society on Urolithiasis Research, the Joint Usage/Research Program of Medical Research Institute, Tokyo Medical and Dental University (to S. Nagamori); Spanish Ministry of Science and Innovation Grant SAF2012-40080-C02-01-FEDER (to M.P.); Spanish Health Institute Carlos III Grant FIS PI13/00121-FEDER (to V.N.); and Generalitat de Catalunya Grants SGR2009-1490 (to V.N.) and SGR2009-1355 (to M.P.).

1. Verrey F, et al. (2004) CATs and HATs: The SLC7 family of amino acid transporters. *Pflugers Arch* 447(5):532–542.
2. Palacín M, Kanai Y (2004) The ancillary proteins of HATs: SLC3 family of amino acid transporters. *Pflugers Arch* 447(5):490–494.
3. Fotiadis D, Kanai Y, Palacín M (2013) The SLC3 and SLC7 families of amino acid transporters. *Mol Aspects Med* 34(2-3):139–158.
4. Kanai Y, et al. (1998) Expression cloning and characterization of a transporter for large neutral amino acids activated by the heavy chain of 4F2 antigen (CD98). *J Biol Chem* 273(37):23629–23632.
5. Chairoungdua A, et al. (1999) Identification of an amino acid transporter associated with the cystinuria-related type II membrane glycoprotein. *J Biol Chem* 274(41): 28845–28848.
6. Feliubadaló L, et al.; International Cystinuria Consortium (1999) Non-type I cystinuria caused by mutations in SLC7A9, encoding a subunit ($b^{0,+}$AT) of rBAT. *Nat Genet* 23(1): 52–57.
7. Chillarón J, et al. (2010) Pathophysiology and treatment of cystinuria. *Nat Rev Nephrol* 6(7):424–434.
8. Pfeiffer R, et al. (1999) Luminal heterodimeric amino acid transporter defective in cystinuria. *Mol Biol Cell* 10(12):4135–4147.
9. Fernández E, et al. (2002) rBAT-$b^{0,+}$AT heterodimer is the main apical reabsorption system for cystine in the kidney. *Am J Physiol Renal Physiol* 283(3):F540–F548.
10. Espino M, et al. (2015) Digenic inheritance in cystinuria mouse model. *PLoS One* 10(9): e0137277.
11. Kanai Y, et al. (1992) Expression of mRNA (D2) encoding a protein involved in amino acid transport in S3 proximal tubule. *Am J Physiol* 263(6 Pt 2):F1087–F1092.
12. Furriols M, et al. (1993) rBAT, related to L-cysteine transport, is localized to the microvilli of proximal straight tubules, and its expression is regulated in kidney by development. *J Biol Chem* 268(36):27060–27068.
13. Feliubadaló L, et al. (2003) Slc7a9-deficient mice develop cystinuria non-I and cystine urolithiasis. *Hum Mol Genet* 12(17):2097–2108.
14. Chillarón J, Roca R, Valencia A, Zorzano A, Palacín M (2001) Heteromeric amino acid transporters: Biochemistry, genetics, and physiology. *Am J Physiol Renal Physiol* 281(6):F995–F1018.
15. Verrey F, Meier C, Rossier G, Kühn LC (2000) Glycoprotein-associated amino acid exchangers: Broadening the range of transport specificity. *Pflugers Arch* 440(4):503–512.
16. Chairoungdua A, et al. (2001) Identification and characterization of a novel member of the heterodimeric amino acid transporter family presumed to be associated with an unknown heavy chain. *J Biol Chem* 276(52):49390–49399.
17. Matsuo H, et al. (2002) Identification of a novel Na^+-independent acidic amino acid transporter with structural similarity to the member of a heterodimeric amino acid transporter family associated with unknown heavy chains. *J Biol Chem* 277(23): 21017–21026.
18. Pfeiffer R, et al. (1999) Amino acid transport of y^+L-type by heterodimers of 4F2hc/CD98 and members of the glycoprotein-associated amino acid transporter family. *EMBO J* 18(1):49–57.
19. Mastroberardino L, et al. (1998) Amino-acid transport by heterodimers of 4F2hc/CD98 and members of a permease family. *Nature* 395(6699):288–291.
20. Khunweeraphong N, et al. (2012) Establishment of stable cell lines with high expression of heterodimers of human 4F2hc and human amino acid transporter LAT1 or LAT2 and delineation of their differential interaction with α-alkyl moieties. *J Pharmacol Sci* 119(4):368–380.
21. Perkins DN, Pappin DJ, Creasy DM, Cottrell JS (1999) Probability-based protein identification by searching sequence databases using mass spectrometry data. *Electrophoresis* 20(18):3551–3567.
22. Peters T, et al. (2003) A mouse model for cystinuria type I. *Hum Mol Genet* 12(17): 2109–2120.
23. Chillarón J, et al. (1997) An intracellular trafficking defect in type I cystinuria rBAT mutants M467T and M467K. *J Biol Chem* 272(14):9543–9549.
24. Bartoccioni P, Rius M, Zorzano A, Palacín M, Chillarón J (2008) Distinct classes of trafficking rBAT mutants cause the type I cystinuria phenotype. *Hum Mol Genet* 17(12):1845–1854.
25. Sakamoto S, et al. (2009) A novel role of the C-terminus of $b^{0,+}$AT in the ER-Golgi trafficking of the rBAT-$b^{0,+}$AT heterodimeric amino acid transporter. *Biochem J* 417(2): 441–448.
26. Nakamura E, et al. (1999) 4F2 (CD98) heavy chain is associated covalently with an amino acid transporter and controls intracellular trafficking and membrane topology of 4F2 heterodimer. *J Biol Chem* 274(5):3009–3016.
27. Garcia ML, Viitanen P, Foster DL, Kaback HR (1983) Mechanism of lactose translocation in proteoliposomes reconstituted with lac carrier protein purified from *Escherichia coli*. 1. Effect of pH and imposed membrane potential on efflux, exchange, and counterflow. *Biochemistry* 22(10):2524–2531.
28. Söderberg O, et al. (2006) Direct observation of individual endogenous protein complexes in situ by proximity ligation. *Nat Methods* 3(12):995–1000.
29. Denayer S, Helsen C, Thorrez L, Haelens A, Claessens F (2010) The rules of DNA recognition by the androgen receptor. *Mol Endocrinol* 24(5):898–913.
30. Kanai Y, Hediger MA (1992) Primary structure and functional characterization of a high-affinity glutamate transporter. *Nature* 360(6403):467–471.
31. Shayakul C, et al. (1997) Localization of the high-affinity glutamate transporter EAAC1 in rat kidney. *Am J Physiol* 273(6 Pt 2):F1023–F1029.
32. Segal S, McNamara PD, Pepe LM (1977) Transport interaction of cystine and dibasic amino acids in renal brush border vesicles. *Science* 197(4299):169–171.
33. Enomoto A, et al. (2002) Molecular identification of a renal urate anion exchanger that regulates blood urate levels. *Nature* 417(6887):447–452.
34. Bailey CG, et al. (2011) Loss-of-function mutations in the glutamate transporter SLC1A1 cause human dicarboxylic aminoaciduria. *J Clin Invest* 121(1):446–453.
35. Di Giacopo A, et al. (2013) Differential cystine and dibasic amino acid handling after loss of function of the amino acid transporter $b^{0,+}$AT (Slc7a9) in mice. *Am J Physiol Renal Physiol* 305(12):F1645–F1655.
36. Kanai Y, Lee WS, You G, Brown D, Hediger MA (1994) The human kidney low affinity Na^+/glucose cotransporter SGLT2: Delineation of the major renal reabsorptive mechanism for D-glucose. *J Clin Invest* 93(1):397–404.
37. Hediger MA, Coady MJ, Ikeda TS, Wright EM (1987) Expression cloning and cDNA sequencing of the Na^+/glucose co-transporter. *Nature* 330(6146):379–381.
38. Brodehl J, Gellissen K, Kowalewski S (1967) [Isolated cystinuria (without lysin-, ornithinand argininuria) in a family with hypocalcemic tetany]. *Monatsschr Kinderheilkd* 115(4):317–320.
39. Stephens AD, Perrett D (1976) Cystinuria: A new genetic variant. *Clin Sci Mol Med* 51(1):27–32.
40. Bovee KC, Thier SO, Rea C, Segal S (1974) Renal clearance of amino acids in canine cystinuria. *Metabolism* 23(1):51–58.
41. Nagamori S, Smirnova IN, Kaback HR (2004) Role of YidC in folding of polytopic membrane proteins. *J Cell Biol* 165(1):53–62.
42. Hagiwara K, et al. (2012) NRFL-1, the C. elegans NHERF orthologue, interacts with amino acid transporter 6 (AAT-6) for age-dependent maintenance of AAT-6 on the membrane. *PLoS One* 7(8):e43050.
43. Biber J, Stieger B, Stange G, Murer H (2007) Isolation of renal proximal tubular brush-border membranes. *Nat Protoc* 2(6):1356–1359.
44. Shigeta Y, et al. (2006) A novel missense mutation of SLC7A9 frequent in Japanese cystinuria cases affecting the C-terminus of the transporter. *Kidney Int* 69(7):1198–1206.
45. Masuda T, Tomita M, Ishihama Y (2008) Phase transfer surfactant-aided trypsin digestion for membrane proteome analysis. *J Proteome Res* 7(2):731–740.
46. Tanaka H, et al. (2012) Linkage of N-cadherin to multiple cytoskeletal elements revealed by a proteomic approach in hippocampal neurons. *Neurochem Int* 61(2): 240–250.
47. Heintzmann R, Cremer CG (1999) Laterally modulated excitation microscopy: Improvement of resolution by using a diffraction grating. *Proc SPIE* 3568:185–196.
48. Bligh EG, Dyer WJ (1959) A rapid method of total lipid extraction and purification. *Can J Biochem Physiol* 37(8):911–917.